

DAMPING OF CORONAL LOOP OSCILLATIONS: CALCULATION OF RESONANTLY DAMPED KINK OSCILLATIONS OF ONE-DIMENSIONAL NONUNIFORM LOOPS

T. VAN DOORSSELAERE, J. ANDRIES, S. POEDTS, AND M. GOOSSENS

Centre for Plasma Astrophysics, Katholieke Universiteit Leuven, Celestijnenlaan 200B, B-3001 Heverlee, Belgium; tomvd@wis.kuleuven.ac.be, jesse.andries@wis.kuleuven.ac.be, stefaan.poedts@wis.kuleuven.ac.be, marcel.goossens@wis.kuleuven.ac.be

Received 2003 May 23; accepted 2004 January 27

ABSTRACT

The analytic study of coronal loop oscillations in equilibrium states with thin nonuniform boundary layers is extended by a numerical investigation for one-dimensional nonuniform equilibrium states. The frequency and the damping time of the ideal kink quasi mode are calculated in fully resistive MHD. In this numerical investigation there is no need to adopt the assumption of a thin nonuniform boundary layer, which is essential for analytic theory. An important realization is that analytical expressions for the damping rate that are equivalent for thin nonuniform layers give results differing by a factor of 2 when they are used for thick nonuniform layers. Analytical theory for thin nonuniform layers does not allow us to discriminate between these analytical expressions. The dependence of the complex frequency of the kink mode on the width of the nonuniform layer, on the length of the loop, and on the density contrast between the internal and the external region is studied and is compared with analytical theory, which is valid only for thin boundaries. Our numerical results enable us to show that there exists an analytical expression for thin nonuniform layers that might be used as a qualitative tool for extrapolation into the regime of thick nonuniform layers. However, when the width of the nonuniform layer is varied, the differences between our numerical results and the results obtained with the version of the analytical approximation that can be extended into the regime of thick nonuniform layers are still as large as 25%.

Subject headings: MHD — Sun: corona — Sun: magnetic fields

1. INTRODUCTION AND MOTIVATION

In 1999, coronal loop oscillations were observed for the first time by the *Transition Region and Coronal Explorer (TRACE)* spacecraft (Aschwanden et al. 1999). Since then, several oscillating loops have been reported and thoroughly studied (Aschwanden et al. 2002; Schrijver, Aschwanden, & Title 2002; Nakariakov et al. 1999).

The observed coronal loop oscillations have been modeled as fast kink oscillations by, e.g., Nakariakov et al. (1999), Ruderman & Roberts (2002), and Goossens, Andries, & Aschwanden (2002) and as phase-mixed torsional Alfvén waves (Ofman & Aschwanden 2002). The rapid damping of the oscillations has been the subject of speculation. Nakariakov et al. (1999) concluded that Reynolds numbers smaller by 8–9 orders of magnitude than the classical value of 10^{14} are needed to explain the rapid damping. A similar conclusion was drawn by Ofman & Aschwanden (2002), who compared several damping mechanisms and, on the basis of the observed periods and damping times, found phase mixing of torsional Alfvén waves to be most likely.

De Pontieu, Martens, & Hudson (2001) computed damping rates of Alfvén waves due to footpoint leakage. Under the assumption that their analysis (for Alfvén waves, basically the analysis of Davila 1991) is also valid for fast waves, De Pontieu et al. (2001) point out that the observed rapid damping can be explained by footpoint leakage within the uncertainties involved in the measurements.

However, Goossens et al. (2002) pointed out that damping by resonant absorption of quasi mode kink oscillations is also a very attractive explanation as, like leakage, it does not require changing the estimates of the Reynolds numbers. Like Ruderman & Roberts (2002), they used the analytical formula for the damping rate, which can be obtained in one-

dimensional models in the classical “thin tube and thin boundary” approximation (TTTB), to calculate the length scales of the inhomogeneity. They concluded that resonant absorption was ruled out by Ofman & Aschwanden, because they did not allow for the radial length scales to vary from loop to loop. Goossens et al. used the observed periods and damping rates combined with analytic results for thin loops with thin nonuniform layers to deduce the width of the nonuniform layer for 11 loops. Most of the values for the width of the nonuniform layers are too large for the TTTB formula to be an accurate approximation. Goossens et al. interpreted this as a motivation for an eigenvalue analysis for one-dimensional nonuniform equilibrium states where the nonuniformity is not restricted to a “thin” layer. Eigenmodes of such highly inhomogeneous loop models have not been calculated before. The observed coronal loop oscillations are a strong impetus for trying to understand damped fast eigenmode oscillations in inhomogeneous models of coronal loops.

Hollweg (1990) used an indirect method to describe the damping of surface waves on “thick” boundaries. By using the width of the resonance curve of the driven problem, they estimated the damping time of the eigenmode. It is unclear whether the relation between the driven problem and the eigenmode problem on which their analysis is based remains unchanged when heavy damping is considered.

The aim of the present paper is to report the results of a direct numerical calculation of resistive eigenmodes in one-dimensional coronal loop models that are highly inhomogeneous, in the sense that the inhomogeneity is not restricted to a “thin” boundary layer. The results are compared with calculations obtained with the “thin boundary” method and with the classical TTTB formula, which in addition assumes that the loops are much longer than they are wide and that the plasma in the loop is uniform.

It is not our purpose to completely imitate a coronal loop up to the finest details. Many details are left out, and crude approximations are made. The aim of this paper is to understand the basic physics without making the unphysical approximation that the boundary layers are thin. The present paper does not embark on a discussion of various oscillation models and damping mechanisms possibly at work in coronal loops. Neither does the present paper intend to carry out a full-scale interpretation and analysis of the observed coronal loop oscillations in terms of resonant absorption. This is done in a separate paper by Aschwanden et al. (2003) in which observational information on the distribution of density in the coronal loops is combined with the numerical results on the oscillations of loops of the present paper to analyze the observed oscillations.

This paper starts with a description of the one-dimensional model and a repetition of the derivation of the classical TTB formula to clearly show the two distinct approximations that are made to obtain that formula. Furthermore, we show that there are several versions of the classical analytical formula that are equivalent in the TTB limit but result in differences up to a factor of 2 when applied in the regime of thick boundaries. In § 6 the resistive kink mode frequencies of one-dimensional highly inhomogeneous coronal loops obtained with the LEDA code (Van der Linden 1991) are presented. The dependence of the damping rate on the free parameters, namely, the inhomogeneity length scale, the loop length, and the density contrast, is investigated.

2. MODEL AND EQUATIONS

We use a straight infinitely long cylindrically symmetric flux tube as a model for the coronal loops. Thus, the curvature of the loop is neglected. This may be justified by the fact that the curvature radius is generally much larger than the radius of the loop. This model is called one-dimensional in the sense that in a system of cylindrical coordinates (r, φ, z) with the z -axis coinciding with the axis of the cylinder (loop), the equilibrium quantities, magnetic field $\mathbf{B} = (0, B_\varphi(r), B_z(r))$, pressure $p(r)$, and density $\rho(r)$ are functions of the radial distance only.

Of course this equilibrium model is a crude model for the equilibrium configuration of coronal loops. *TRACE* shows that coronal loops have a filamentary structure with a complicated two-dimensional (or even three-dimensional) distribution of the density. The present one-dimensional equilibrium model contains the basic physics causing the damping of oscillations in coronal loops. The basic physics is the spatial variation of the density and hence the local Alfvén speed, which causes MHD waves to be resonantly damped. The spatial variation of the local Alfvén velocity is more complicated in realistic two-dimensional or three-dimensional equilibria, and hence the damping of the oscillations for these equilibrium models is more difficult to compute, but the same physical principle is at work. As a matter of fact, the results for the oscillations of a simple one-dimensional cylindrical model seem to agree rather well with the observations (Aschwanden et al. 2003). It is reassuring that the physical mechanism causing the damping is captured with this simple one-dimensional equilibrium model.

The magnetic field and the pressure satisfy the radial force balance equation

$$\frac{d}{dr} \left(p + \frac{B^2}{2\mu} \right) = -\frac{B_\varphi^2}{\mu r}. \quad (1)$$

This equation does not involve density, so the density profile can be chosen freely. Since the plasma pressure is much smaller than the magnetic pressure in the corona, it is a good first approximation to neglect plasma pressure. This classical $\beta = 0$ approximation removes the slow magnetosonic waves from the analysis. When the magnetic field is straight, $\mathbf{B} = B(r)\mathbf{e}_z$, equation (1) also implies that the magnetic field is constant. The coronal loop is then a density enhancement in a homogeneous field. Thus, this object is very different from photospheric and solar interior flux tubes, which are concentrations of magnetic field surrounded by field free plasma of higher density.

Since the equilibrium quantities depend on r only, the perturbed quantities can be Fourier analyzed with respect to the negligible coordinates φ and z and set proportional to $\exp(i(m\varphi + k_z z))$. Here m (an integer) and k_z are the azimuthal and axial wavenumbers. Similarly, we can propose the following time dependence: $\exp(-i\omega t)$, where ω is the angular frequency. Since we use complex frequencies for which the imaginary part describes the damping of the wave amplitude, the appropriate mathematical approach is to use a Laplace transform rather than a Fourier transform.

The relevant equations for the linear motions of a pressureless plasma superposed on a static one-dimensional cylindrical equilibrium model with a straight magnetic field are

$$\begin{aligned} \rho v_A^2 (\omega^2 - \omega_A^2) \frac{d(r\xi_r)}{dr} &= - \left[(\omega^2 - \omega_A^2) - \frac{m^2}{r^2} v_A^2 \right] r P', \\ \frac{dP'}{dr} &= \rho (\omega^2 - \omega_A^2) \xi_r \end{aligned} \quad (2)$$

(e.g., Appert, Gruber, & Vaclavik 1974), where ξ is the displacement, P' is the Eulerian perturbation of the total pressure, $v_A = B/(\mu\rho)^{1/2}$ is the Alfvén speed, and $\omega_A = k_z v_A$ is the Alfvén frequency. Although the displacements of the loops seen in the *TRACE* movies are large, linear perturbation theory may still be valid. To investigate this, the radial velocity should be compared with a typical speed of the plasma and not with the equilibrium value, which is 0 in our case. Taking numbers from Aschwanden et al. (2002), we obtain Alfvén Mach numbers, all smaller than 6%. This is a good indication that linear perturbation theory can still be used.

3. SOLUTIONS FOR DISCONTINUOUS MODELS

Equations (2) admit analytical solutions in terms of (modified) Bessel's functions for uniform equilibrium models. When used for coronal loops, these uniform cylindrical equilibrium models are characterized by a true discontinuity surface where the equilibrium quantities vary from their constant internal to their constant external values. The true discontinuity is situated at $r = R$, and R is the loop radius. By combining the two first-order equations (2), one second-order equation for P' can be obtained that for constant equilibrium quantities reduces to the modified Bessel's equation

$$\frac{d^2 P'}{dr^2} + \frac{1}{r} \frac{dP'}{dr} - \left(\frac{m^2}{r^2} + \kappa^2 \right) P' = 0,$$

with

$$\kappa^2 = -\frac{\omega^2 - \omega_A^2}{v_A^2}. \quad (3)$$

For the internal region, the solutions obeying the regularity condition at the axis are

$$\begin{aligned} P'_i &= AI_m(\kappa_i r), \\ \xi_{ri} &= A \frac{\kappa_i}{\rho_i(\omega^2 - \omega_{Ai}^2)} I'_m(\kappa_i r). \end{aligned} \quad (4)$$

For the external region, the solutions have to vanish at infinity (at least for real κ) so that

$$\begin{aligned} P'_e &= BK_m(\kappa_e r), \\ \xi_{re} &= B \frac{\kappa_e}{\rho_e(\omega^2 - \omega_{Ae}^2)} K'_m(\kappa_e r). \end{aligned} \quad (5)$$

I_m and K_m are the modified Bessel's functions of order m of the first and second kind, respectively. The prime denotes the derivative with respect to the argument, and κ is defined as the square root with the positive real part of κ^2 . However, when $\omega > \omega_{Ae}$, κ^2 is real and negative. The waves are then propagating in the external medium. The appropriate boundary condition to impose then is that waves are carrying energy away from the tube. In that case the waves become damped because of the leakage of energy. In that situation the root should be taken differently, as damped outgoing waves have unbounded amplitude at infinity. A discussion on this topic can be found in Andries & Goossens (2001, 2002). We do not have to worry about this as we do not consider leaky waves any further.

The dispersion relation is obtained by matching the internal and external solutions. At the discontinuous boundary, both ξ_r and P' have to be continuous. This leads to the dispersion relation

$$D(\omega, m, k_z) \equiv \frac{\xi_{re}(r=R)}{P'_e(r=R)} - \frac{\xi_{ri}(r=R)}{P'_i(r=R)} = 0,$$

which with the above analytical expressions becomes

$$\frac{\kappa_i}{\rho_i(\omega^2 - \omega_{Ai}^2)} \frac{I'_m(\kappa_i R)}{I_m(\kappa_i R)} = \frac{\kappa_e}{\rho_e(\omega^2 - \omega_{Ae}^2)} \frac{K'_m(\kappa_e R)}{K_m(\kappa_e R)} \quad (6)$$

(Edwin & Roberts 1983).

The dispersion relation can be solved numerically for general m , k_z , and R . From the Bessel's functions in equation (4), we can see that oscillations that displace the axis of the tube necessarily have the azimuthal wavenumber $m = 1$. Thus, the observed oscillations of coronal loops have to be interpreted as fundamental kink modes. Since there are no nodes along the tube, we can furthermore express the longitudinal wavenumber as $k_z = \pi/L$, where L is the length of the coronal loop.

As κ roughly scales with k_z (see eq. [3]), the arguments of the Bessel's functions become small when the tube is long compared with its radius $L \gg R$. For small arguments, we can approximate $I'_m(z)/I_m(z) \approx m/z$ and $K'_m(z)/K_m(z) \approx -m/z$ except for $m = 0$ where $I'_0(z)/I_0(z) \approx z/2$ and $K'_0(z)/K_0(z) \approx -1/(z \ln z)$. Thus, in the "thin tube" or "long tube" approximation the dispersion relation for all $m \neq 0$ modes becomes

$$D = -\frac{m}{R} \left[\frac{1}{\rho_e(\omega^2 - \omega_{Ae}^2)} + \frac{1}{\rho_i(\omega^2 - \omega_{Ai}^2)} \right] = 0, \quad (7)$$

which can readily be solved to yield the well-known result

$$\omega = \sqrt{\frac{\rho_i \omega_{Ai}^2 + \rho_e \omega_{Ae}^2}{\rho_i + \rho_e}} = k_z B \sqrt{\frac{2}{\rho_i + \rho_e}}. \quad (8)$$

In the thin tube approximation (TT) the frequencies of the eigenoscillations are independent of the azimuthal wavenumber m . An exception is the sausage mode ($m = 0$), in which no long-wavelength limit can be obtained. For small tubes the sausage mode becomes leaky.

4. SOLUTIONS FOR A "THIN" NONUNIFORM BOUNDARY LAYER

Analytical solutions to equations (2) do not exist in general for nonuniform equilibrium models. The dispersion relation cannot be written down in closed analytical form, except possibly for special choices of the equilibrium profiles. Analytic progress is still possible when the true discontinuity is replaced with a thin nonuniform boundary layer $[R - l/2, R + l/2]$ of thickness l in which the equilibrium quantities vary continuously from their constant internal to their constant external values. A thin nonuniform layer (TB) means that $l/R \ll 1$. The outer radius of the loop is now $a = R + l/2$, but since $l/R \ll 1$, $a \approx R$. Similarly, the inner radius of the loop $b = R - l/2 \approx R$. It could be anticipated that the variations in the nonuniform boundary layer can be neglected as long as l is small compared with the length scale of the variations in expressions (4) and (5). However, this is not true. Because of the singularity in equations (2), large variations occur in the nonuniform boundary layer. In fact, as is the case for kink mode oscillations, for real frequencies in the Alfvén continuum $[\omega_{Ai}, \omega_{Ae}]$ the amplitude becomes unbounded where $\omega = \omega_A(r)$. The Alfvén continuum is a continuous range of eigenfrequencies because for these frequencies the solution obeying the right boundary condition always matches the solution obeying the left boundary condition as they get unbounded at the resonant position (Goedbloed 1983). When dissipation is taken into account, the singularity is removed, and the variations around the resonance can be obtained analytically by a local asymptotic analysis. For the driven problem, this was done by Sakurai, Goossens, & Hollweg (1991); Goossens, Hollweg, & Sakurai (1992); Goossens, Ruderman, & Hollweg (1995); and Erdelyi, Goossens, & Ruderman (1995). The eigenvalue problem was treated by Tirry & Goossens (1996). The variations in the resonant layer can be expressed as jump conditions over the resonant layer:

$$\begin{aligned} [P'] &= 0, \\ [\xi_r] &= -\pi l \frac{m^2/r_0^2}{\rho_0 |\Delta_A|} P'. \end{aligned} \quad (9)$$

The subscript 0 indicates that the quantities are evaluated at the Alfvén resonant surface (thus, r_0 indicates the position of the resonant surface), and Δ_A stands for the derivative of ω_A^2 . In a plasma with constant magnetic field, we can rewrite $|\Delta_A|$:

$$\begin{aligned} \rho_0 |\Delta_A| &= \rho_0 (k_z^2 B^2) \frac{1}{\rho_0^2} \left| \frac{d\rho}{dr}(r_0) \right| \\ &= \omega_0^2 \frac{|\rho_i - \rho_e|}{l} \alpha, \end{aligned} \quad (10)$$

where

$$\alpha = \frac{l}{|\rho_i - \rho_e|} \left| \frac{d\rho}{dr}(r_0) \right|$$

is the slope of the density profile normalized to the width of the layer and to the total density difference. It is a parameter that depends only on the shape of the density profile.

The jump conditions are independent of the values of the magnetic diffusivity and the viscosity. In fact, they can even be obtained in ideal MHD by analytical continuation of the solutions into the lower half of the complex frequency plain (Vanlommel et al. 2002). This is effectively equivalent to studying the analytical continuation of the Green's function when solving the initial value problem (Lee & Roberts 1986; Goedbloed 1983 in planar geometry; Ruderman & Roberts 2002 for kink modes in cylindrical geometry). The analytical continuation of the dispersion relation obtained this way yields complex roots that cannot be eigenfrequencies of the Hermitian differential operator. Therefore, they are called quasi modes. These quasi modes are the natural oscillation modes of the system (Balet, Appert, & Vaclavik 1982; Steinolfson & Davila 1993) and correspond to eigenmodes in dissipative MHD in the limit of vanishing resistivity and viscosity (Poedts & Kerner 1991; Tirry & Goossens 1996).

Taking into account the variations around the resonance (eqs. [9]) while ignoring all other variations in the nonuniform boundary layer, we can write the dispersion relation as

$$D(\omega) = -\pi i \frac{lm^2/r_0^2}{\omega_0^2 |\rho_i - \rho_e| \alpha}, \quad (11)$$

where $i^2 = -1$. We then search for solutions in the neighborhood of the solution for the discontinuous model $\omega = \omega_0 + \delta\omega$ and develop $D(\omega)$ in a Taylor series to find the imaginary frequency shift

$$\delta\omega = -\frac{\pi lm^2/r_0^2}{\omega_0^2 |\rho_i - \rho_e| \alpha [\partial D(\omega_0)/\partial \omega]} i. \quad (12)$$

Note that $D(\omega)$ is a complex function. However, since ω_0 is real and $D(\omega)$ is real for real arguments, the Cauchy-Riemann conditions ensure that the derivative is real. Thus, the resulting frequency shift $\delta\omega$ is purely imaginary. The procedure to find quasi mode frequencies in the “thin boundary” (TB) approximation thus goes as follows. The dispersion relation (6) is solved numerically and yields the real part of the frequency. On the basis of the real part of the frequency, the resonant position is determined, and equation (12) is used to calculate the frequency shift.

An analytic expression for the damping rate can be obtained when the “thin tube” and “thin boundary” approximations are combined. By using equations (7) and (8) to approximate $\partial D(\omega_0)/\partial \omega$, the frequency correction becomes

$$\delta\omega_i = -\pi \frac{m}{8\alpha} \left(\frac{R}{r_0}\right)^2 \frac{l}{R} \left(\frac{|\rho_i - \rho_e|}{\rho_i + \rho_e}\right) \omega_0. \quad (13)$$

Ruderman & Roberts write their corresponding equation in terms of l/a . Since $l/R \ll 1$ and $a = R + l/2$, the difference between the two formulas is second order, and therefore they are equivalent in the TB approximation. Likewise, $R \approx r_0$. We thus obtain

$$\frac{\delta\omega_i}{\omega_0} = -\frac{\pi m l}{8\alpha R} \frac{|\rho_i - \rho_e|}{\rho_i + \rho_e}. \quad (14)$$

This relation shows that under TTTB the damping rate is linearly proportional to the length scale of the inhomogeneity l/R . It was first obtained by Hollweg & Yang (1988) for nearly perpendicular propagation of a surface wave on a Cartesian interface. Hollweg & Yang applied the result to coronal loops

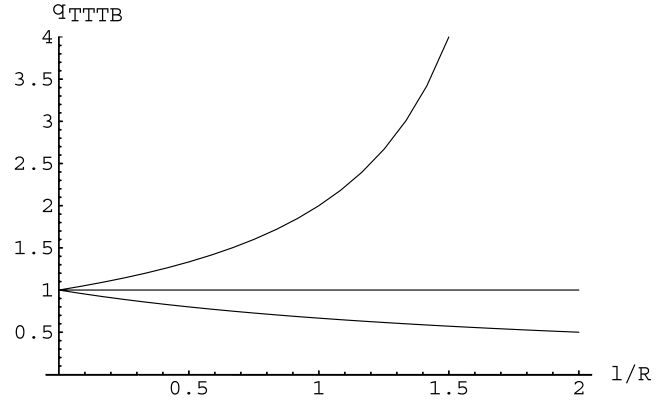


FIG. 1.—Predicted dependence of the normalized damping rate q_{TTTB} on l/R : linear dependence on l/b (top curve), linear dependence on l/R (middle curve), linear dependence on l/a (bottom curve).

as the limit of nearly perpendicular propagation in Cartesian geometry coincides with the “thin tube” limit in cylindrical geometry. More than a decade before the oscillations were observed, they concluded that oscillations of coronal loops would be damped effectively with an e -folding time of two periods. Hence, Hollweg decay is a good name for referring to this phenomenon of heavily damped coronal loop oscillations. This result was also obtained by Goossens et al. (1992) and recently retrieved by Ruderman & Roberts (2002), who related it to the observed damping of coronal loop oscillations. They used the observed period and damping time of a coronal loop oscillation to estimate the inhomogeneity length scale. As Goossens et al. (2002) did the exercise for a data set of 11 events obtained by Aschwanden et al. (2002), it became clear that the formula is pushed beyond its limit. The values for the inhomogeneity length scale are between 0.15 and 0.5 and out of the TTTB range.

We already noted that Ruderman & Roberts derived linear dependence on l/a . Similarly, we could equally well derive linear dependence on l/b . However, note that

$$\frac{l}{a} = \frac{l}{R + l/2} = \frac{l}{R} \frac{1}{(1 + l/2R)},$$

$$\frac{l}{b} = \frac{l}{R - l/2} = \frac{l}{R} \frac{1}{(1 - l/2R)},$$

so linear variation with l/R does not imply linear variation with l/a nor with l/b . This illustrates very clearly that the linear dependence is valid only within the TB range, i.e., $l/R \ll 1$, where the three formulas converge. Figure 1 shows how very strongly the three possible formulas, which are equally valid in the TB limit, diverge when l/R becomes larger; e.g., for $l/R = 0.75$ the damping obtained from the linear dependence on l/b is twice that obtained from the linear dependence on l/a . In its simplicity this is an important observation. It tells us that analytical expressions that are equivalent for thin nonuniform layers when extended to thick nonuniform layers give results differing by a factor of 2. The message is that quantitative conclusions on quasi mode damping of coronal loop oscillations require quasi mode frequencies to be computed for conditions outside the TTTB range. At this point it is not clear whether there actually exists an analytical expression for qualitative information that can be extended with some confidence into the regime of thick nonuniform layers. It is important to realize that analytical

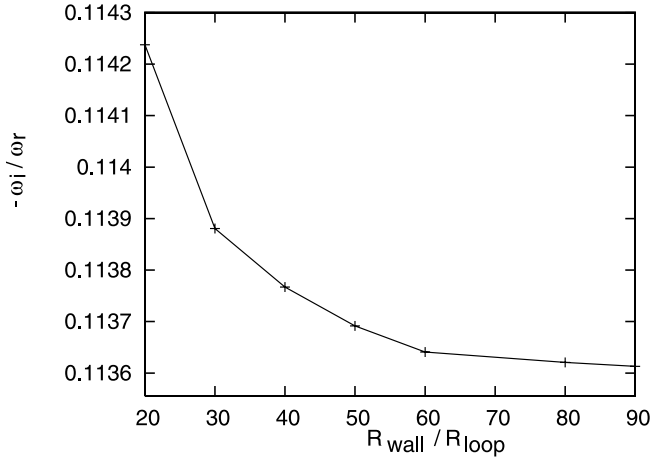


FIG. 2.—Influence of the boundary for $k_z = 0.02$, $l/R = 1$, and $\zeta = 10$. The vertical axis shows $-\omega_i/\omega_r$, and the horizontal axis shows the distance of the wall normalized with respect to the radius of the loop.

theory for thin nonuniform layers cannot provide this information. Our numerical results show that qualitatively the linear dependence on l/R (not on l/a or l/b) can be extrapolated for thick boundaries, although quantitative differences of up to 25% occur.

5. SOLUTIONS FOR HIGHLY NONUNIFORM MODELS

The calculation of quasi modes for one-dimensional highly nonuniform models is much more involved. This is not primarily due to the thickness of the inhomogeneous layer itself. A numerical integration routine could be used to integrate the set of differential equations (2) away from the resonance. While the jump conditions or the analytical dissipative solutions could be used to cross the resonant layer, this method was used by Tirry & Goossens (1995) and Tirry, Aschwanden, & Title (1997). The real problem resides in the fact that the damping increases as the nonuniform layer becomes thicker. Instead of using the Taylor expansion, a numerical root finder has to be used to obtain the solutions of equation (11). The tricky part is that the jump relations (9) are derived for weak damping and cannot be generalized easily to strong damping.

Hollweg (1990) used an indirect method in which the width of the resonance curve of the driven problem was used to estimate the damping of a surface wave. It is uncertain, however, whether this simple relation between the width of the resonance curve and the damping time, which was proved to exist for weak damping, remains true for strong damping.

In the case of strong damping, we then need to solve the dissipative MHD equations numerically. For that purpose we use the LEDA code (Large-scale Eigenvalue solver for the Dissipative Alfvén spectrum). This code was originally developed by Van der Linden (1991) to calculate the linear resistive spectrum for a one-dimensional equilibrium with flow in a tokamak fusion reactor. The equilibrium configuration consists of a cylindrical plasma surrounded by a vacuum and a perfectly conducting wall. The program uses a finite-element method to discretize the linearized MHD equations. By applying the appropriate boundary conditions, the problem is reduced to an algebraic eigenvalue problem, which is solved by a standard algebraic technique, e.g., a QR algorithm or Jacobi-Davidson iteration (van der Holst et al. 1999).

To model the dense coronal loops surrounded by an infinite low-density plasma, the vacuum is removed. Moreover, to

avoid influencing the results, the (unphysical) wall should be positioned sufficiently far away in comparison with the radial length scales of the perturbation. As can be seen on Figure 2, the (complex) frequency of the kink mode becomes independent of the distance of the wall when the wall is sufficiently far away. Figure 2 was obtained for a worst-case scenario ($k_z = 0.02$). As all the observed oscillating loops (Aschwanden et al. 2002) are shorter (have larger k_z), it can be anticipated that the radial length scales are smaller and thus that the boundary is effectively farther away. In further calculations we have placed the wall at $50R$, resulting in errors less than 0.1%.

6. RESULTS

According to equation (1), the density profile can be chosen freely. We follow Ruderman & Roberts (2002) and take a sinusoidal variation of density characterized by the four quantities ρ_i , ρ_e , R , and l as

$$\begin{aligned} \rho &= \rho_i \text{ for } 0 \leq r < R - \frac{l}{2}, \\ \rho &= \frac{\rho_i}{2} \left[\left(1 + \frac{1}{\zeta}\right) - \left(1 - \frac{1}{\zeta}\right) \sin \frac{\pi}{l}(r - R) \right] \\ &\text{for } R - \frac{l}{2} \leq r \leq R + \frac{l}{2}, \\ \rho &= \rho_e \text{ for } r > R + \frac{l}{2}, \end{aligned} \quad (15)$$

where ρ_i is the density of the inner core of the loop, ρ_e is the density of the external uniform plasma in which the tube is embedded, $\zeta = \rho_i/\rho_e$, l is the length scale of the variation of the equilibrium density, and $a = R + l/2$ is the outer radius of the loop, while $b = R - l/2$ is the inner radius and R is the mean radius. With this profile α becomes $\pi/2$ in the TTTB approximation, and it is close to it in the “thin boundary” approximation (but varying with ω_r). Note that equation (15) is written in terms of the density contrast ζ , which is the inverse of the Ruderman & Roberts density ratio χ . With our definition of ζ , the density contrast always takes values larger than 1 for overdense coronal loops, and the density contrast really becomes larger when ζ increases. This density profile mimics a straight overdense coronal loop embedded in an infinitely extending homogeneous plasma. The enormous complexity revealed by the *TRACE* movies suggests that the ambient plasma is not homogeneous. As a result, coronal loops probably interact with other nearby loop threads. The investigation of these interactions is beyond the scope of this paper. In contrast with Ruderman & Roberts (2002), we do not insist that the nonuniform layer is thin. For a fully nonuniform equilibrium without a uniform inner core, $R = l/2$ and $l = a$. All length scales (thus also the longitudinal wavenumbers) are normalized to R . In particular, we use equation (13) with the factor l/R rather than the Ruderman & Roberts equation with the factor l/a . For thin boundary layers, it does not matter whether we use l/R or l/a . For thick nonuniform layers, we prefer to use l/R since R is a better approximation of the position of the resonance. This is a simple operation, which turns out to be of key importance. Our numerical results show that the analytical expression using l/R turns out to provide a relatively accurate extension into the regime of thick nonuniform layers. Magnetic fields are normalized to the strength of the homogeneous magnetic field pointing in the z -direction, densities to the internal density ρ_i , and times to

Alfvén crossing times. We focus on $-\omega_i/\omega_r$, which is a dimensionless observable quantity and not affected by the performed normalization. In particular, we want to know how far the linear dependence on l/R remains true when the boundary layer gets thicker. Therefore, we often normalize ω_i/ω_r with respect to the value that is obtained by extrapolation of the linear TTTB formula and thus express our results in terms of the quantity q_{TTTB} :

$$-\frac{\omega_i}{\omega_r} = -q_{\text{TTTB}} \frac{1}{4} \frac{l}{R} \frac{\zeta - 1}{\zeta + 1}.$$

The free parameters in the problem are l/R , k_z , and ζ . The parameter ranges $l/R \in [0.1; 2]$ and $k_z \in [0.02; 0.18]$ are chosen in such a way that all the coronal loops observed by Aschwanden et al. (2002) are covered. Aschwanden (2001) found values of $\zeta \in [8; 18]$ for loops with strong flux contrast, while the density contrast of the oscillating loops analyzed in Aschwanden et al. (2003) was found to be weaker. We therefore take $\zeta \in [1.5, 20]$. In what follows, the frequency and the damping rate of the kink mode have been calculated in three different ways. In the first method, we have used the classical analytic theory in which it is explicitly assumed that the nonuniform layer is thin and the tube is very long, as in TTTB (formulas [8] and [14]). It is clear that this method is used out of its range of validity when applied to real loops. In the second method, we have used the jump relations (9) for weak damping to compute the damping rate. As explained, the jump relations are accurate only for small damping (and hence, thin nonuniform boundary layers), but we used them anyway to cross general nonuniform layers (formulas [6] and [12]), as in TB. It is clear that this method as well is used out of its range of validity when applied to real loops. In the third method, we computed the frequency and the damping rate with the eigenvalue code LEDA.

6.1. Convergence in η

In Figure 3 $-\omega_i/\omega_r$ is plotted versus $-\log \eta$. It is clear that for sufficiently small resistivity η , the damping becomes independent of the resistivity. In this regime, the damping rate tends to the damping rate of the ideal quasi mode (as shown by Poedts & Kerner 1991). However, for very small η the convergence breaks down because of numerical errors. The thickness of the resonant layer scales with $\eta^{1/3}$ (see, e.g., Tirry

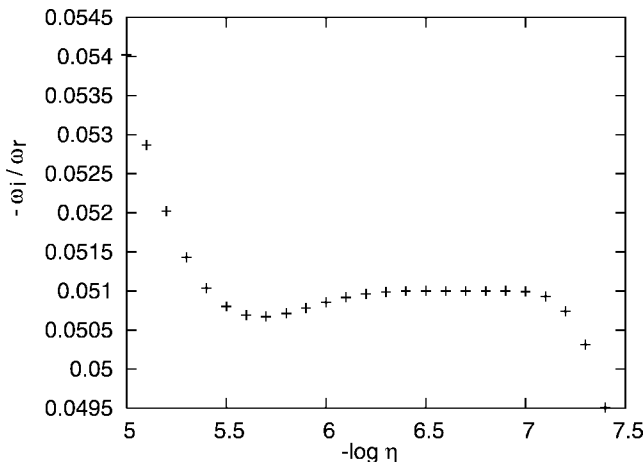


FIG. 3.—Dependency on η . The horizontal axis shows the value of $-\log \eta$, while the vertical axis shows the value of $-\omega_i/\omega_r$. The plot is made with $\zeta = 10$, $k_z = 0.16$, and $l/R = 1$.

& Goossens 1996). When η becomes too small, there are not enough grid points to resolve the resonant layer. This induces numerical errors, which can be reduced by incorporating more grid points. For specified k_z , l/R , ζ , and a certain number of grid points, we can choose a value for the resistivity small enough to assure that the damping is independent of the resistivity but large enough that the number of grid points suffices to resolve the dissipative layer. We find that value of the resistivity increases when l/R becomes larger (and the other parameters remain constant). This can be expected because the ideal damping of the quasi mode gets stronger for larger l/R , and the extra resistive damping can be neglected in comparison with the ideal damping rate.

6.2. l/R -Dependency

As emphasized by equation (14), analytic theory for a thin nonuniform layer predicts that ω_i/ω_r is a linear function of l/R (the normalized boundary layer width) and also of $(\rho_i - \rho_e)/(\rho_i + \rho_e) = (\zeta - 1)/(\zeta + 1)$. An important objective of the present paper is to determine to what extent the dependence of ω_i/ω_r on l/R deviates from linearity for highly nonuniform equilibrium states.

The dependency on l/R of the results found with the use of the three methods is illustrated in Figures 4 and 5. On Figure 4 we have plotted $4(\omega_i/\omega_r)(\zeta + 1)/(\zeta - 1) = q_{\text{TTTB}}(l/R)$ as a function of l/R . The damping rate is thus normalized with respect to the TTTB damping rate, except for the linear l/R -factor. The TTTB formula (14) is therefore represented by the first bisector. Figure 5 shows $4(\omega_i/\omega_r)[(\zeta + 1)/(\zeta - 1)](R/l) = q_{\text{TTTB}}$ versus l/R , i.e., the damping rate normalized to the TTTB damping rate. The TTTB results are thus a horizontal line. First of all note that, for small k_z (which means very thin coronal loops), the TB approximation almost coincides with the TTTB theory. This was to be expected as the TTTB theory is the limit of the TB approach for $k_z \rightarrow 0$. For larger k_z (Fig. 5, *bottom*) the thin boundary approximation deviates slightly from the straight line of the TTTB theory. For small l/R the approximate TTTB and the approximate TB results do not differ very much from the correct LEDA results. For larger values of k_z (Fig. 5, *bottom*) the LEDA results tend to the TB curve rather than the TTTB curve. This illustrates again that the TB method uses only $l/R \rightarrow 0$, while the TTTB theory in addition assumes $k_z \rightarrow 0$. The LEDA results start to deviate significantly (over 5%) when l/R is about 0.5. For intermediate l/R (around 1) a maximum difference of almost 20% can be observed. For larger values of l/R the difference diminishes and eventually disappears again. For extremely large values of l/R (fully inhomogeneous model), TTTB theory, as well as the TB method, overestimates the damping rate calculated by LEDA. In this region a deviation up to 25% can be calculated. Figure 5 should be compared with Figure 1. This comparison shows clearly that the LEDA results differ much less with the linear l/R dependence than with the linear l/b or l/a dependence. Hence, our preference is to compare with the l/R formula that thus can be extrapolated into the regime of thick nonuniform layers with an accuracy of 25%.

6.3. k_z -Dependency

To illustrate the k_z -dependency of the damping rate q_{TTTB} , we plot the normalized damping rate versus k_z for fixed ζ and l/R (Fig. 6). For small k_z the approximate TTTB results and the approximate TB results differ only slightly from one another. For $l/R \rightarrow 1.0$ the approximate TTTB results and the

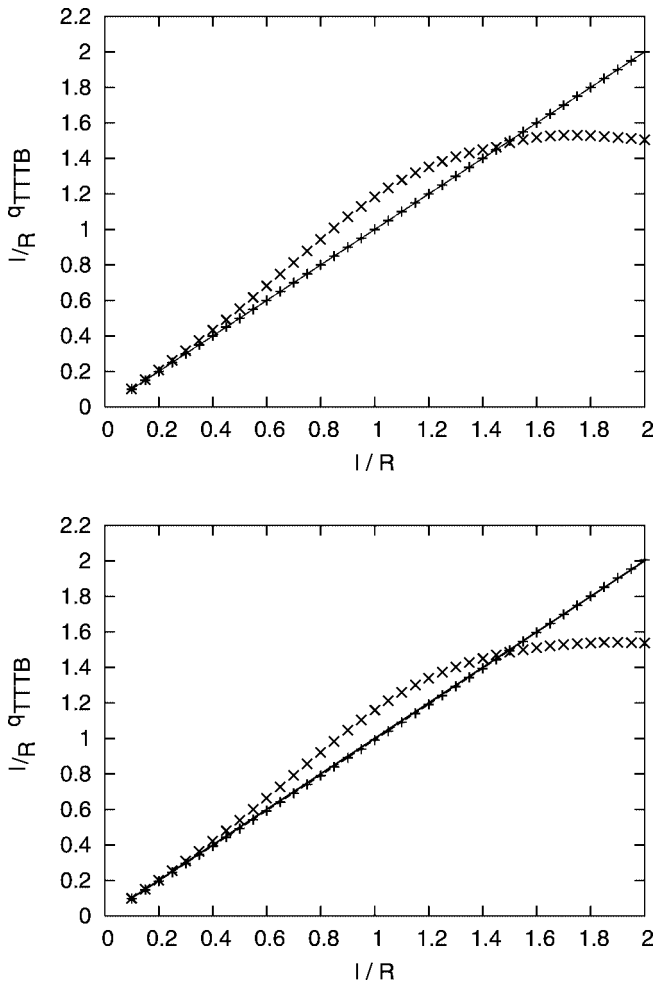


FIG. 4.—Dependency on l/R . The horizontal axis shows l/R , while the vertical axis shows the normalized damping rate $(l/R)q_{TTTB}$. Both figures are for $\zeta = 3$. *Top*, Dependency for $k_z = 0.02$; *bottom*, dependency for $k_z = 0.18$. The solid line shows TTTB, the dashed line shows the TB approach, and the unconnected crosses indicate the frequencies found by LEDA.

approximate TB results differ substantially from those found by LEDA. However, just like the TB results, the damping seems to become weaker for shorter loops.

6.4. Combined l/R - and k_z -Dependency

We plot in Figure 7 q_{TTTB} versus l/R and k_z , while keeping ζ constant at 3. The upper surface is defined by the LEDA results; the lower surface is defined by the TB results. The TTTB theory is shown by a horizontal $q_{TTTB} = 1$ plane. Figure 7 seems to be characterized by a strong decrease of the ratio q_{TTTB} for the LEDA results, when l/R increases beyond 1.

Because we are looking at a combined effect of ω_i and ω_r , we want to see which of them causes the decrease in the damping rate for larger values of l/R . In Figure 8, we plot ω_r normalized to the TTTB result (formula [8]) versus l/R and k_z for a constant $\zeta = 3$. Figure 8 shows that the approximate TTTB results and the approximate TB results for the frequency deviate substantially from the correct LEDA results for $l/R > 1$. To visualize the large increase of ω_r we make a cut of the three-dimensional surface for $k_z = 0.1$. As can be seen on Figure 9, this large increase cannot completely explain the decrease of the damping rate visible in Figure 7.

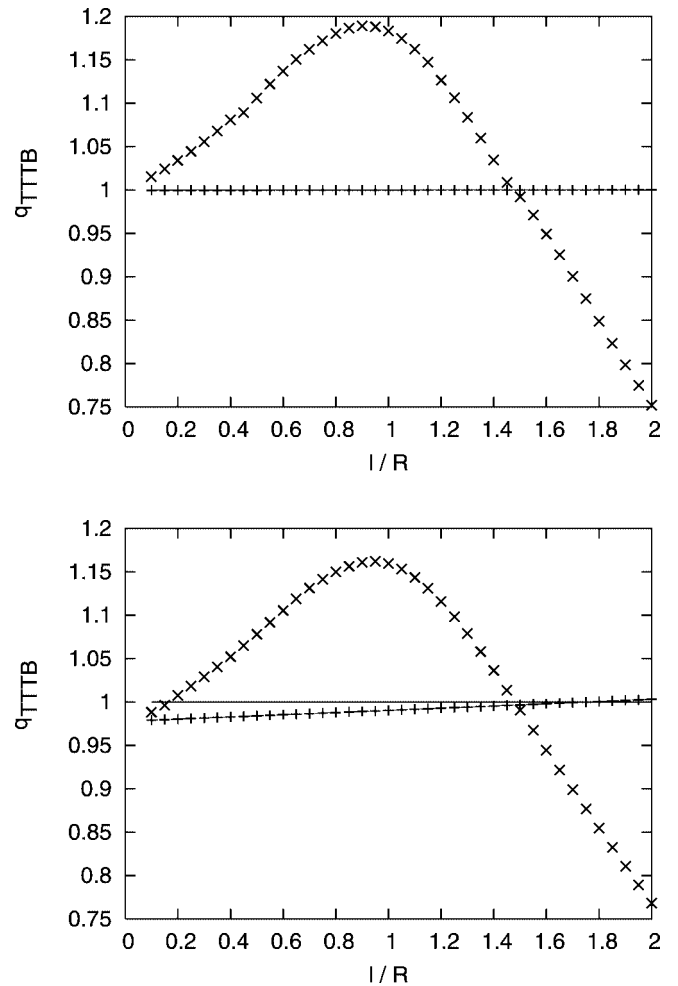


FIG. 5.—Same as Fig. 4, except for a different normalization of the damping rate. The vertical axis represents q_{TTTB} .

6.5. ζ -Dependency

In Figure 10 we plot the normalized damping rate q_{TTTB} versus ζ while keeping l/R and k_z constant. For large density contrasts ($\zeta > 6$), the three methods produce nearly constant but different values. Hence, it is clear that the TTTB results describe very well the ζ -dependency of the damping rate. As

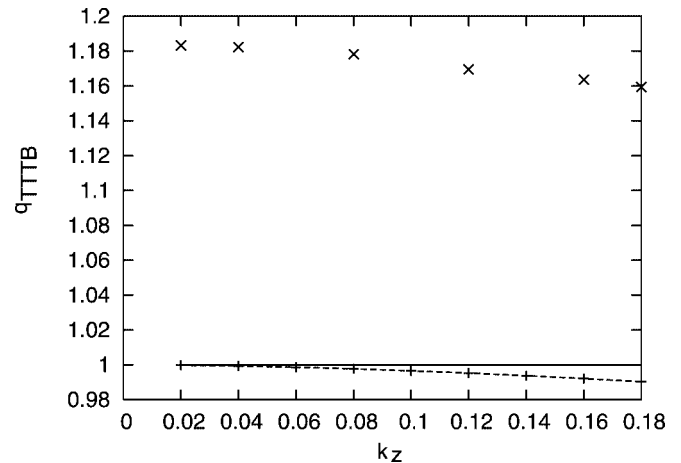


FIG. 6.—Dependency on k_z . The horizontal axis shows k_z , while the vertical axis shows the normalized damping rate, q_{TTTB} . The figure is for $\zeta = 3$ and $l/R = 1.0$. The symbols are the same as in Fig. 4.

in Figure 6, the vertical spacing between the LEDA and the other results is caused by the different l/R -behavior. However, for smaller ζ , the ζ -dependency of the TTTB formula overestimates the damping rates (when compared with the values for larger ζ). Figure 11 shows the combined dependency of the results on ζ , k_z , and l/R . From these figures it is clear that the TTTB ζ -dependency breaks down when ζ tends to 1.

7. SUMMARY AND DISCUSSION

In this paper we have studied the kink mode oscillations in one-dimensional cylindrical models of magnetic coronal loops by the LEDA numerical code. First we have pointed out that analytical expressions for the damping rate that are equivalent for thin nonuniform layers can give widely differing results when used for thick nonuniform layers. We have stressed that analytical theory for thin nonuniform layers cannot help here. Our numerical results have enabled us to show that the analytical expression using l/R allows a relatively accurate extension into the regime of thick nonuniform layers. R is not the radius of the loop but rather the midpoint of the nonuniform layer. Once this analytical expression using l/R was identified as a plausible point of reference, we have compared our numerical results with those obtained by the TB method (which assumes that $l/R \rightarrow 0$) and the TTTB method (which in addition assumes that $k_z \rightarrow 0$).

From this comparison it is clear that for large ζ , the ζ -dependency is more or less explained by the TTTB method. Large deviations occur only for small ζ .

The k_z -dependency of the LEDA results is, apart from a vertical shift due to the l/R -dependency, approximately explained by the TB approach. A smaller damping rate can be expected when shorter loops are considered.

As expected for small l/R (up to 0.5), the LEDA results follow the TTTB approximation. However, for larger values

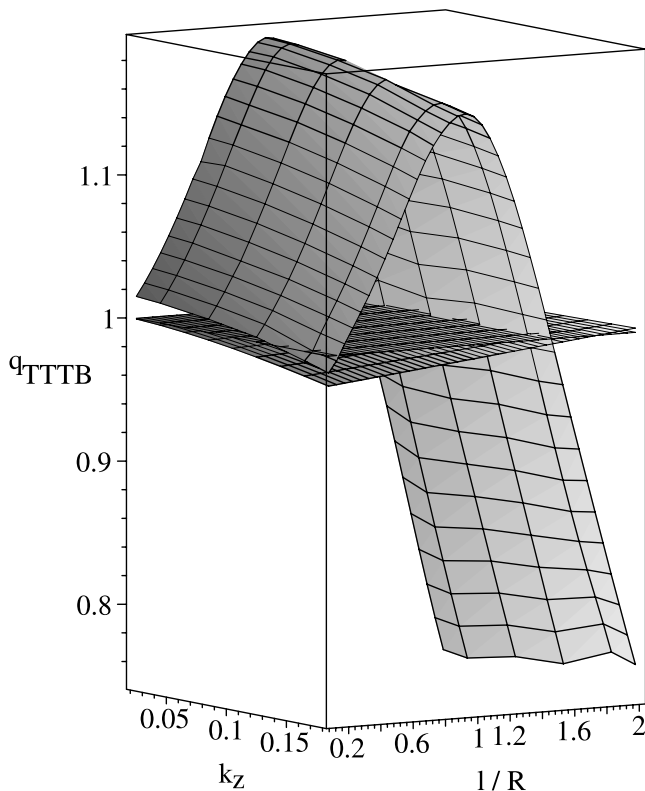


FIG. 7.—Dependency of ω_i/ω_r on l/R and k_z ($\zeta = 3$)

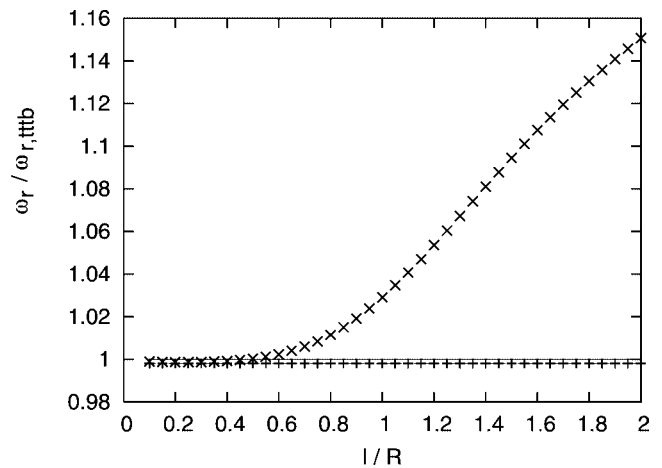
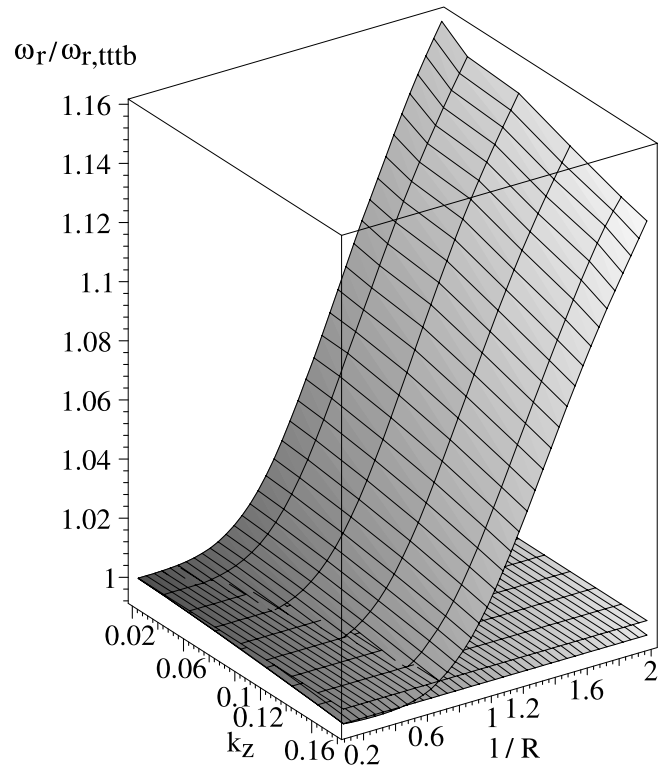


FIG. 8.—Top: Dependency of the normalized ω_r on l/R and k_z . The vertical axis shows the normalized real part of the frequency. Bottom: Cut of the top graph for $k_z = 0.08$. The figures are both for $\zeta = 3$.

of $l/R \approx 1$, the damping rate is underestimated by almost 20% by the TTTB formula. When l/R increases even further, this difference diminishes again. When $l/R \approx 2$ (fully inhomogeneous model), the LEDA damping rate is overestimated by 25% by the TTTB formula.

In this way, the calculated LEDA curves resemble those obtained by Hollweg (1990) for the l/R -dependency of the damping of the ideal quasi mode. Another resemblance to Hollweg's results is the LEDA curve for the kink frequency, which exhibits the same behavior when l/R is small enough. Only when l/R becomes larger than 1 is there a significant difference in the behavior.

From our numerical calculations, it is clear that, as Goossens et al. (2002) argued, the high damping rates observed in solar coronal loop oscillations can easily be explained by resonant

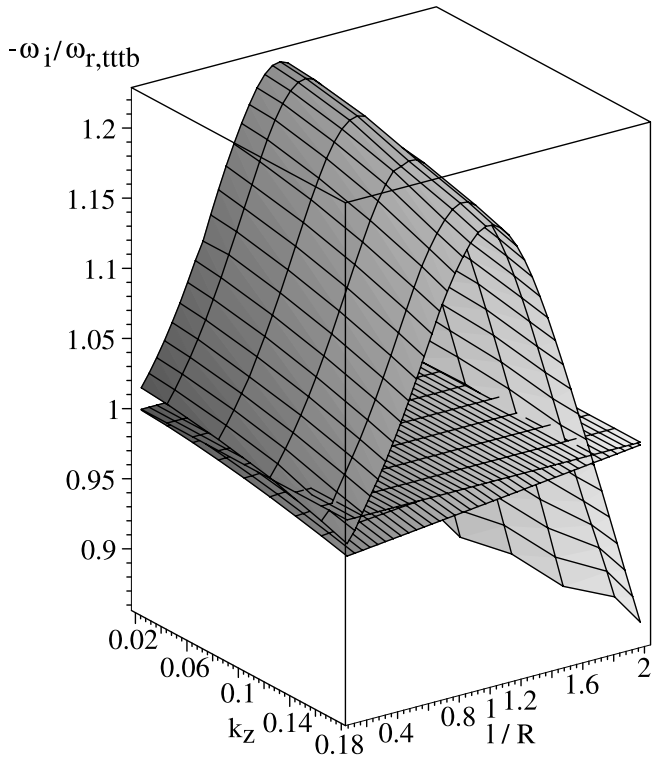
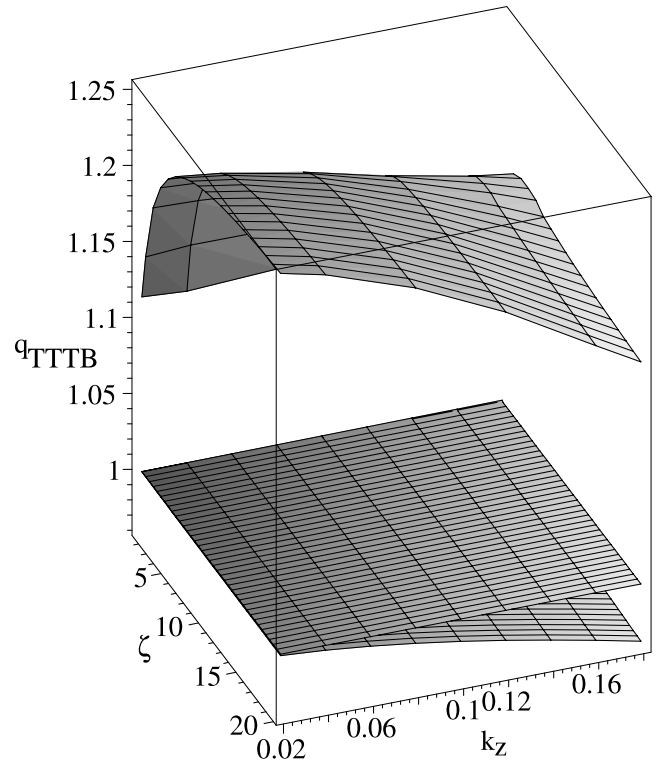


FIG. 9.—Dependency of the normalized $\omega_i/\omega_{r,TTTB}$ on l/R and k_z . The figure is for $\zeta = 3$.



absorption, when large inhomogeneity length scales are taken into account. There is no need to adopt smaller Reynolds numbers. An important finding of the present paper is that for low-density contrasts and large inhomogeneity length scales, as observed in oscillating coronal loops (Aschwanden et al. 2003), the numerical computed damping rates can deviate by up to 25% from the approximate results predicted by the simple thin boundary formula.

With the present results, as in helioseismology, a frequency inversion can be performed when an oscillating coronal loop has been observed. From the observed quantities (loop length and density contrast), we can calculate an approximation for the Alfvén speed and, when the density is known, for the magnetic field. The results of the present eigenvalue computations

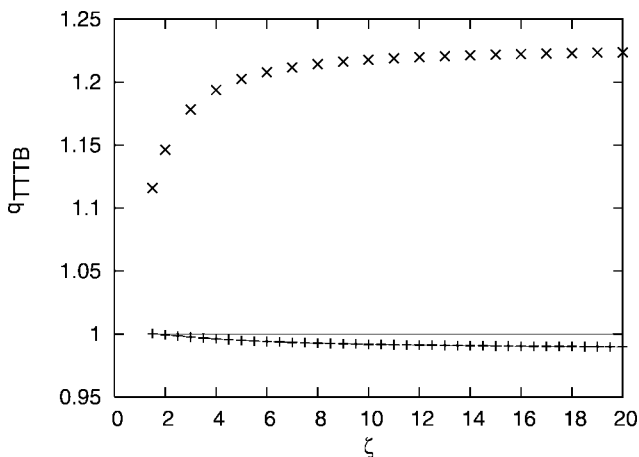


FIG. 10.—Dependency on ζ . The horizontal axis shows ζ , while the vertical axis shows the normalized damping rate. The figure is for $k_z = 0.08$ and $l/R = 1.0$. The symbols are the same as in Fig. 4.

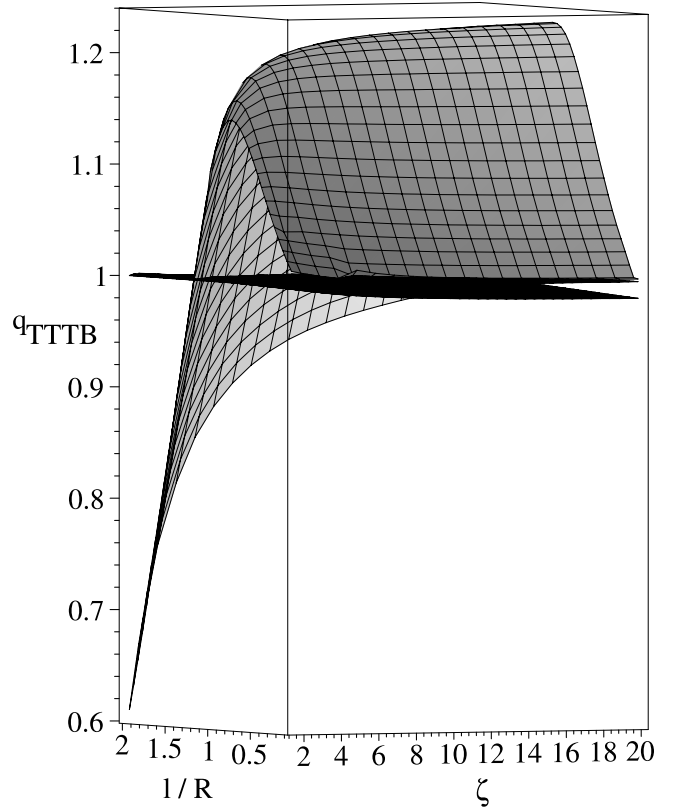


FIG. 11.—Top: Dependency of ω_i/ω_r on ζ and k_z . The figure is for $l/R = 1$. Bottom: Dependency of ω_i/ω_r on ζ and l/R . The figure is for $k_z = 0.08$.

have been used by Aschwanden et al. (2003) for investigating a set of coronal loop oscillations observed by *TRACE*.

In that article the density contrast is calculated from the observed damping time and compared with the observed density contrast. In spite of the crudeness of the model, the agreement between the observed and calculated density contrast is within a factor of 3, which is remarkably small given the large observational restraints. It is reassuring that the physical mechanism causing the damping, namely, the resonant damping due to the spatial variation of the Alfvén speed, is captured with this simple one-dimensional equilibrium model.

A point that is left out in the present analysis and needs to be considered in future has to do with the boundary conditions in the axial direction. At the footpoints no boundary condition is explicitly imposed. The standing wave is just obtained as a superposition of two propagating waves running in opposite directions along the tube. The footpoint leakage is not taken into account. Since the equilibrium model is nonuniform only in the radial direction, the effect of the rapid decrease in density from the photosphere into the chromosphere and corona cannot be taken into account either. Footpoint leakage contributes to the damping of the fast kink mode oscillations. A correct treatment of footpoint leakage on fast kink mode oscillations requires a full two-dimensional equilibrium model with stratification in the radial and axial directions. Footpoint leakage has so far been studied only for torsional ($m = 0$) Alfvén

waves in cylindrical flux tubes (Hollweg 1984; Davila 1991; Berghmans & de Bruyne 1995; De Pontieu et al. 2001). All these studies, with the exception of Berghmans & de Bruyne (1995), have an equilibrium model with constant density in the radial direction and a variable density in the axial direction. Berghmans & de Bruyne (1995) take a two-dimensional distribution of the equilibrium density. De Pontieu et al. (2001) apply the result obtained by Davila (1991) for torsional Alfvén waves to fast kink waves in coronal loops and conclude that footpoint leakage can explain the observed rapid damping. Fast mode kink oscillations have not yet been computed in the presence of footpoint leakage. The combined effect of resonant absorption and footpoint leakage on the damping of fast kink oscillations requires the study of two-dimensional equilibrium models. It is known that both footpoint leakage and resonant absorption damp the fast oscillations. But there are no quantitative results for the damping of fast kink oscillations by footpoint leakage. Neither is it known how resonant absorption and footpoint leakage interact. Here we have concentrated on the damping by resonant absorption alone.

The authors would like to acknowledge Ronald Van der Linden, who originally developed the LEDA code, as well as all others who perfected it. In particular, we thank Bart van der Holst for his technical assistance concerning the code.

REFERENCES

- Andries, J., & Goossens, M. 2001, *A&A*, 368, 1083
 ———. 2002, *Phys. Plasmas*, 9, 2865
 Appert, K., Gruber, R., & Vaclavik, J. 1974, *Phys. Fluids*, 17, 1471
 Aschwanden, M. J. 2001, *ApJ*, 560, 1035
 Aschwanden, M. J., De Pontieu, B., Schrijver, C. J., & Title, A. M. 2002, *Sol. Phys.*, 206, 99
 Aschwanden, M. J., Fletcher, L., Schrijver, C. J., & Alexander, D. 1999, *ApJ*, 520, 880
 Aschwanden, M. J., Nightingale, R., Andries, J., Goossens, M., & Van Doorselaere, T. 2003, *ApJ*, 598, 1375
 Balet, B., Appert, K., & Vaclavik, J. 1982, *Plasma Phys.*, 24, 1005
 Berghmans, D., & de Bruyne, P. 1995, *ApJ*, 453, 495
 Davila, J. M. 1991, in *Mechanisms of Chromospheric and Coronal Heating*, ed. P. Ulmschneider, E. R. Priest, & R. Rosner (Berlin: Springer), 464
 De Pontieu, B., Martens, P. C. H., & Hudson, H. S. 2001, *ApJ*, 558, 859
 Edwin, P. M., & Roberts, B. 1983, *Sol. Phys.*, 88, 179
 Erdelyi, R., Goossens, M., & Ruderman, M. S. 1995, *Sol. Phys.*, 161, 123
 Goedbloed, J. P. 1983, *Lecture Notes on Ideal Magnetohydrodynamics* (Rijnhuizen Rep. 83-145; Nieuwegein Assoc. Euratom-FOM)
 Goossens, M., Andries, J., & Aschwanden, M. J. 2002, *A&A*, 394, L39
 Goossens, M., Hollweg, J. V., & Sakurai, T. 1992, *Sol. Phys.*, 138, 233
 Goossens, M., Ruderman, M. S., & Hollweg, J. V. 1995, *Sol. Phys.*, 157, 75
 Hollweg, J. V. 1984, *ApJ*, 277, 392
 ———. 1990, *J. Geophys. Res.*, 95, 2319
 Hollweg, J. V., & Yang, G. 1988, *J. Geophys. Res.*, 93, 5423
 Lee, M. A., & Roberts, B. 1986, *ApJ*, 301, 430
 Nakariakov, V. M., Ofman, L., DeLuca, E. E., Roberts, B., & Davila, J. M. 1999, *Science*, 285, 862
 Ofman, L., & Aschwanden, M. J. 2002, *ApJ*, 576, L153
 Poedts, S., & Kerner, W. 1991, *Phys. Rev. Lett.*, 66, 2871
 Ruderman, M. S., & Roberts, B. 2002, *ApJ*, 577, 475
 Sakurai, T., Goossens, M., & Hollweg, J. V. 1991, *Sol. Phys.*, 133, 227
 Schrijver, C. J., Aschwanden, M. J., & Title, A. M. 2002, *Sol. Phys.*, 206, 69
 Steinolfson, R. S., & Davila, J. M. 1993, *ApJ*, 415, 354
 Tirry, W. J., Cadez, V. M., & Goossens, M. 1997, *A&A*, 324, 1170
 Tirry, W. J., & Goossens, M. 1995, *J. Geophys. Res.*, 100(A12), 23687
 ———. 1996, *ApJ*, 471, 501
 van der Holst, B., Beliën, A., Goedbloed, J., Nool, M., & van der Ploeg, A. 1999, *Phys. Plasmas*, 6, 1554
 Van der Linden, R. 1991, Ph.D. thesis, Katholieke Univ. Leuven
 Vanlommel, P., Debosscher, A., Andries, J., & Goossens, M. 2002, *Sol. Phys.*, 205, 1